

# The human dynamic clamp as a paradigm for social interaction

Guillaume Dumas<sup>a,1</sup>, Gonzalo C. de Guzman<sup>a</sup>, Emmanuelle Tognoli<sup>a</sup>, and J. A. Scott Kelso<sup>a,b,1</sup>

<sup>a</sup>The Human Brain and Behavior Laboratory, Center for Complex Systems and Brain Sciences, Florida Atlantic University, Boca Raton, FL 33431; and <sup>b</sup>Intelligent Systems Research Centre, University of Ulster, Derry ~ Londonderry BT48 7JL, Northern Ireland

Edited\* by Michael I. Posner, University of Oregon, Eugene, OR, and approved July 17, 2014 (received for review April 23, 2014)

Social neuroscience has called for new experimental paradigms aimed toward real-time interactions. A distinctive feature of interactions is mutual information exchange: One member of a pair changes in response to the other while simultaneously producing actions that alter the other. Combining mathematical and neurophysiological methods, we introduce a paradigm called the human dynamic clamp (HDC), to directly manipulate the interaction or coupling between a human and a surrogate constructed to behave like a human. Inspired by the dynamic clamp used so productively in cellular neuroscience, the HDC allows a person to interact in real time with a virtual partner itself driven by well-established models of coordination dynamics. People coordinate hand movements with the visually observed movements of a virtual hand, the parameters of which depend on input from the subject's own movements. We demonstrate that HDC can be extended to cover a broad repertoire of human behavior, including rhythmic and discrete movements, adaptation to changes of pacing, and behavioral skill learning as specified by a virtual "teacher." We propose HDC as a general paradigm, best implemented when empirically verified theoretical or mathematical models have been developed in a particular scientific field. The HDC paradigm is powerful because it provides an opportunity to explore parameter ranges and perturbations that are not easily accessible in ordinary human interactions. The HDC not only enables to test the veracity of theoretical models, it also illuminates features that are not always apparent in real-time human social interactions and the brain correlates thereof.

human-machine interface | artificial agent |  
 computational social neuroscience | multiscale | dynamical systems

Reciprocally coupled complex systems in biology and psychology are notoriously difficult to study. Over the course of the last three decades, understanding how real neurons work individually and together has grown significantly in large part due to the so-called dynamic clamp paradigm (see ref. 1 for a review). The initial idea was to combine a standard electrophysiological setup with a computer interface, and then control in real time the current injected into a neuron as a function of its membrane potential measured via an intracellular electrode (2). The original dynamic clamp used tried and tested electrophysiological models such as the Hodgkin-Huxley equations (3) to explore parametrically how neurons behave. The latter, considered one of the most significant accomplishments in biophysics in the 20th century, provides a quantitative description of the electric potential across a cell membrane. The interaction between the real neuron and its artificial counterpart allows simulating artificial membrane or synaptic conductance (4, 5), chemical or electronic inputs (6, 7), and even connections with other neurons (8). Because the dynamic clamp falls midway between computational modeling and experimental electrophysiology, it affords the same degree of precision and freedom at the modeling level, while keeping the complexity of interaction with real neurons intact.

Might a similar approach be scaled up or down (as the case may be) to other levels of description? For example, were a human to interact with a model constructed to behave like him- or herself, might this tell us something about human beings and how they

work together? Social neuroscience has increasingly emphasized the need for new experimental paradigms, specifically for the case of real-time social interactions (9). Were it available, a human dynamic clamp (HDC) would provide an opportunity to explore parameter ranges and perturbations that are beyond the reach of traditional experimental designs involving live interactions. However, scaling the paradigm from neurons and neural ensembles to human beings and human brains in a principled fashion is nontrivial. A potential starting point is to ground the design of an HDC in the empirically based theoretical models of coordination dynamics (10).

In what follows, we will describe the HDC for four classes of behavior. Basically, the HDC models the interactions between a human and a virtual partner (VP) in the language of informationally coupled, nonlinear dynamical systems. The movements of the human enter the equations of motion associated with a specific model. This produces the dynamics of the VP that are displayed on a video screen. To complete the reciprocal coupling between the human and VP, the subject sees the motion of the VP. In a first version, the rhythmic movements of the subject enter the equations of motion of the Haken-Kelso-Bunz (HKB) model (11), considered one of the most extensively tested quantitative models of human motor behavior (12–14). Then, we expand the behavioral repertoire of the VP through the excitator model (14–16), which describes both rhythmic and discrete movement generation. In a further elaboration, adaptive behavior is introduced through changing parameter dynamics (17), illustrated here by modifying the intrinsic frequency of the VP (18). Finally, to study how a VP may adopt a directed behavior and hence play the role of a "teacher," we use an adaptation of the empirically

## Significance

The human dynamic clamp (HDC) is proposed as a general paradigm for studies of elementary forms of social behavior in complex biological systems. HDC enables parametric control of real-time bidirectional interaction between humans and empirically grounded theoretical models of coordination dynamics. It thus provides necessary experimental access for laboratory investigations, while preserving the reciprocity and open boundary conditions inherent in daily life social interactions. As proof of concept, different implementations are illustrated, ranging from coordination of rhythmic and discrete movements to adaptive and directed behaviors. The HDC may be a powerful tool for blending theory and experiment at different levels of description, from neuronal populations to cognition and social behavior.

Author contributions: G.D., G.C.d.G., E.T., and J.A.S.K. designed research; G.D., G.C.d.G., E.T., and J.A.S.K. performed research; G.D., E.T., and J.A.S.K. analyzed data; and G.D., E.T., and J.A.S.K. wrote the paper.

The authors declare no conflict of interest.

\*This Direct Submission article had a prearranged editor.

Freely available online through the PNAS open access option.

<sup>1</sup>To whom correspondence may be addressed. Email: dumas@ccs.fau.edu or kelso@ccs.fau.edu.

This article contains supporting information online at [www.pnas.org/lookup/suppl/doi:10.1073/pnas.1407486111/-DCSupplemental](http://www.pnas.org/lookup/suppl/doi:10.1073/pnas.1407486111/-DCSupplemental).

verified Schöner–Kelso model of behavioral pattern change (ref. 19, but see also refs. 20–22).

The validity of all four realizations of the HDC is established by showing empirical results that confirm the existence of a dynamic coordination between humans and VPs, akin to the concept of generalized synchronization in physics (23). Our results suggest that if adequate models of behavior exist for different tasks and functions, and if a medium for two-way interaction and information exchange is available, a deeper understanding of emergent forms of social coordination may ensue. Crucially, demonstrating dynamical coordination between human and VP allows one to infer that both the coupling between the human and VP and the internal dynamics of the VP are appropriate models for the human observer. This allows one to explore a range of parameters and dynamical architectures that support meaningful interaction from a human perspective.

## Methods

**Subjects.** Ten naïve subjects (three female and seven male, 18–60 y old) provided written informed consent and participated in the interactions with the HDC. Procedures were approved by the Internal Review Board at Florida Atlantic University and conformed to the principles expressed in the Declaration of Helsinki. All subjects were right handed and had normal or corrected-to-normal vision. None of them reported a history of neurological or psychiatric disorder.

**Apparatus.** Human participants were seated in front of a computer monitor placed in a sound-isolated room (Fig. 1). Their left hand rested on a table and the right index finger was placed in a manipulandum that rotated freely in the transverse (horizontal) plane about a fixed axis aligned with the metacarpophalangeal joint (Fig. 1, Lower Left). The movement of the finger (angular displacement), transduced by a DC potentiometer, was digitized with a National Instruments analog-to-digital converter at a sampling rate of 500 Hz.

**Software.** Movement data (red “y” in Fig. 1) were fed into a real-time C++ multithread software program (Fig. 1, Right). Velocity of human movement (red  $\dot{y}$  in Fig. 1) was numerically computed using a three-point differentiation algorithm and digitized along with the position data. All of the differential equations were integrated using a Runge–Kutta fourth-order algorithm at 500 Hz, leading to a maximum delay of 2 ms between acquisition and computation of the model output. Model position (blue x in Fig. 1) was used to select one of 119 position-indexed images, which were displayed on the screen (Fig. 1, Upper Left). The screen animation was refreshed at 120 Hz during the experiment and looked just like a normal video of a moving hand.

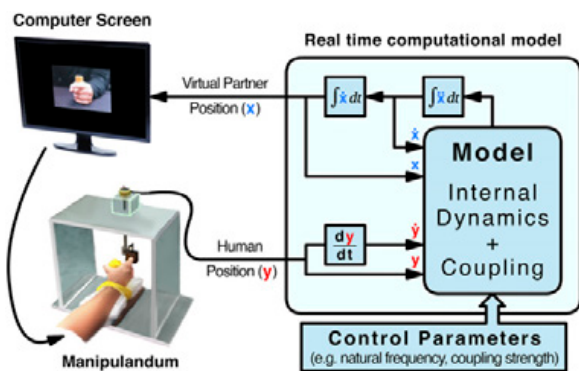


**Fig. 1.** Schematic of the HDC. Human subjects coordinate finger movements with a VP displayed on a computer screen. The subject’s finger position and velocity (state variables) are used as input to the coupling term of the model system (Table 1). The instantaneous position and velocity of the animated finger movements of the VP are determined from a real-time numerical simulation of the model equations that drive the display. The coupling is bidirectional: The subject is visually coupled to the model via the display, and the subject’s own movements (via the coupling) affect the display. Control parameters can be fixed, e.g., as in model 1, or change adaptively in time, as in model 3.

**Models Implemented.** The HDC models the interactions between a subject and a VP as a bidirectionally coupled dynamical system. Any implementation of the HDC thus contains two main parts: the intrinsic dynamics of the model and its coupling with the human. The HDC implemented here covers continuous (rhythmic), discrete, adaptive, and directed behavior (see Table 1 for a summary). It is worth noting that each model has a strong empirical basis and that successive models are mathematical generalizations of their antecedents, not simply independently formalized functional modules.

**Model 1: Rhythmic Behavior.** The first version of the HDC embeds one of the most studied and quantitatively tested models of human movement behavior—the HKB model—into the context of real-time human social interaction (24). The original form of the HKB equations describes and predicts the coordination dynamics of two rhythmically moving components and their functional interaction (11). Many studies have shown that the relative phase  $\phi$  is a relevant collective variable that captures the coordination between two rhythmically moving components. The HKB model provides the equations of motion for both the relative phase and the nonlinear interaction between the components (25). At the collective level, the HKB model reads as

$$\dot{\phi} = -a \sin(\phi) - 2b \sin(2\phi), \quad [1]$$

where  $\phi$  is the relative phase between the human and the VP, the dot signifies the derivative with respect to time, and  $a$  and  $b$  are parameters whose main effects are to control the coupling strength and attractor landscape (for more details, see ref. 26). The VP is endowed with a behavior of its own and, by means of coupling, with the further capacity to coordinate movement with a human (Fig. 1).

At the component level, the relevant state variables are no longer the relative phases but individual finger position and velocity. Hence, the HDC dynamics is

$$\ddot{x} + (\alpha x^2 + \beta \dot{x}^2 - \gamma) \dot{x} + \omega^2 x = (A + B(x - \mu y)^2) (\dot{x} - \mu \dot{y}), \quad [2]$$

where  $x$  and  $y$  represent respectively VP and human finger position, the dots the derivatives,  $\alpha$ ,  $\beta$ , and  $\gamma$  are control parameters such as stiffness and damping associated with empirically measured properties of human movement (e.g., refs. 27 and 28),  $\omega$  is the movement frequency,  $A$  and  $B$  are coupling parameters between the VP and the human, and  $\mu$  is a constant fixed to either +1 or –1, indicating the preference or goal of the VP for inphase or antiphase coordination (see Fig. 3).

**Model 2: Discrete Behavior.** Experiments show that discrete and rhythmic movements can be distinguished based on their phase flow topology (13, 14). Both kinds of movements can be modeled with a single theoretical model, the so-called excitator (15). The excitator defines a universal class of 2D dynamical systems able to exhibit limit cycles for rhythmic movement, and fixed-point dynamics for posture and discrete movements. Not only does the excitator offer a parsimonious way to explain discrete and continuous behaviors with the same dynamical system, it also provides novel predictions regarding phenomena such as false starts that have been confirmed experimentally (16).

Excitator behavior is constrained by three topological characteristics of the phase flow: the boundedness of the trajectory; the existence of a separatrix marking the boundary between two separate regimes; and the existence of attractors, stable fixed point(s) for monostable and bistable discrete movements, and a limit cycle regime for rhythmic movements. Implementing the excitator in the HDC, the equations read

$$\begin{cases} \dot{x}_1 = \omega(x_1 + x_2 - g_1(x_1))\tau \\ \dot{x}_2 = -\omega(x_1 - a + g_2(x_1, x_2) - l)/\tau, \end{cases} \quad [3]$$

with

$$g_1(x_1) = \frac{1}{3}x_1^3 \quad \text{and} \quad g_2(x_1, x_2) = -bx_2, \quad [4]$$

where  $x_1$  and  $x_2$  are the variables with their derivatives ( $x_1$  and  $x_2$  relating to fast and slow dynamics, respectively),  $\omega$  is the frequency of the VP,  $a$  and  $b$  control the location and angle of the separatrix,  $l$  represents an input, and  $\tau$  is a time constant. Notice that the choice of the functions  $g_1$  and  $g_2$ , although not fixed, must nevertheless guarantee the boundedness of the system so that it belongs to the universal class of self-excitable systems.

**Table 1. Overview of the equations and key parameters that govern the four theoretical models embedded in the HDC**

Behavior	Model	Equation(s): internal dynamics = coupling		Key parameters
		Internal dynamics	Coupling*	
Rhythmic coordination	Original version of HKB (11)	$\ddot{x} + (\alpha x^2 + \beta \dot{x}^2 - \gamma)\dot{x} + \omega^2 x$	$(A + B(x - \mu y)^2)(\dot{x} - \mu \dot{y})$	Intrinsic frequency ( $\omega$ ), Van der Pol ( $\alpha$ ), Rayleigh ( $\beta$ ), damping ( $\gamma$ ), and coupling ( $A$ and $B$ )
Rhythmic and discrete movement	Excitator-adapted Jirsa–Kelso (15)	$\begin{cases} \dot{x}_1 = \omega(x_1 + x_2 - g_1(x_1))\tau \\ \dot{x}_2 = \frac{-\omega(x_1 - a + g_2(x_1, x_2) - l)}{\tau} \end{cases}$ with $g_1(x_1) = \frac{1}{3}x_1^3$ and $g_2(x_1, x_2) = -bx_2$	Same as above	Angle and location of the nullclines ( $a$ and $b$ ) and time constant ( $\tau$ )
Frequency adaptation	Dynamic Hebbian learning-adapted Righetti et al. (18)	Either of the above	$\dot{\omega} = \nu(\omega_0 - \omega) \pm \kappa F(t) \frac{x_2}{\sqrt{x_1^2 + x_2^2}}$	Strength of the adaptation ( $\kappa$ ), preferred frequency ( $\omega_0$ ), and strength of the preference ( $\nu$ )
Directed coordination	Virtual teacher-adapted Schöner–Kelso (19) <sup>†</sup>	Either of the above	$-c(\cos(\psi)(\dot{x} - \dot{y}) + \sin(\psi)\omega y)$	Intended relative phase ( $\psi$ ) and strength of the intention ( $c$ )

See *Models Implemented*. Note that starting with HKB (top row) each model builds upon the one before it thereby developing an increasingly fuller picture of dynamic coordination.

\* $x$  and  $\dot{x}$  correspond to the state variables of the VP, and  $y$  and  $\dot{y}$  are the equivalent variables for the human participant.

<sup>†</sup>See *SI Appendix* for details.

The two first-order equations for  $x_1$  and  $x_2$  (Eq. 3) are converted to a unidimensional second-order equation by eliminating  $x_2$  to give a similar form to Eq. 2:

$$\ddot{x} + \tau\omega \left( \frac{\delta g_1}{\delta x} - 1 \right) + \omega^2 \left( x - a - g_2 \left( x, \frac{\dot{x}}{\tau\omega} - x + g_1(x) - l \right) \right) = (A + B(x - y)^2)(\dot{x} - \dot{y}). \quad [5]$$

To incorporate the excitator model into the HDC, we substitute the  $g_1$  and  $g_2$  functions and obtain

$$\ddot{x} + \tau\omega(x^2 + x^4 - 1) + \omega^2 \left( x - a - b \left( \frac{\dot{x}}{\tau\omega} - x + \frac{1}{3}x^3 + \frac{1}{5}x^5 - l \right) \right) = (A + B(x - y)^2)(\dot{x} - \dot{y}). \quad [6]$$

One can immediately recognize on the right-hand side of Eq. 6 the nonlinear coupling already used in the HKB model (where  $y$  refers to the human behavior). This coupling still holds here and causes either convergence or divergence of the trajectories in the phase space. Because trajectories are bounded, constraints lead to inphase or antiphase modes of coordination, respectively (for further details, see ref. 15).

**Model 3: Adaptive Behavior.** Adaptation relies on parameter dynamics according to the scale of observation (17). Implementing frequency adaptation in the HDC thus appears to be a good first step to investigate the parameter dynamics necessary to more fully understand human adaptive behavior. Different strategies for modeling frequency adaptation exist in the literature. For example, in currently popular Bayesian approaches, frequency adaptation is error based and relies on reinforcement learning (e.g., ref. 29). In predictive coding, the adaptation of model parameters is associated with Hebbian and synaptic plasticity (30). Other bottom-up strategies—mostly along the lines of connectionist models—have been developed in the fields of signal processing (31) and robotics (32). Here we follow the strategy of coordination dynamics. Such a dynamical approach has accounted for many phenomena such as frequency adaptation in fireflies (33) and tempo adaptation in musical rhythms (34). A nice aspect of the resulting HDC is that frequency adaptation emerges spontaneously from the interaction of human and VP.

Following Righetti et al. (18, 35), we introduce frequency adaptation into the HDC by transforming the parameter  $\omega$  into a new state variable, with its own time-dependent dynamics:

$$\begin{cases} \dot{x}_1 = f_{x_1}(x_1, x_2, \omega) + F(t) \\ \dot{x}_2 = f_{x_2}(x_1, x_2, \omega) \end{cases} \quad \text{and} \quad \dot{\omega} = \nu(\omega_0 - \omega) \pm \kappa F(t) \frac{x_2}{\sqrt{x_1^2 + x_2^2}}, \quad [7]$$

where  $\kappa$  is the coupling strength,  $(x_1, x_2)$  are the state variables of the oscillator in Cartesian coordinates and  $F(t)$  is the time periodic perturbation caused by the human participant. We also introduce  $\omega_0$  as the preferred frequency of the HDC and a relaxation parameter  $\nu$ . The sign in front of  $\kappa$  depends on the rotation direction in the 2D phase space of the HDC  $(x_1, x_2)$ . The addition of frequency adaptation to the HDC is compatible with both the HKB and excitator models.

**Model 4: Directed Behavior.** Behavior is often directed toward a specific goal. In the theory of coordination dynamics, to modify or change the system's behavior, new information—say a task to be learned or an intention to change behavior—is expressed in terms of parameters acting on the system-relevant variables and their dynamics. The benefit of identifying the latter is that one knows what to modify to produce behavioral change (36). Both empirical and theoretical work shows that intentional forcing is capable of parameterizing the dynamics, e.g., by destabilizing/stabilizing a target pattern of coordination (e.g., refs. 19, 20, 37, and 38) and that neurophysiologically the basal ganglia play a key role (22). Following Schöner and Kelso (19) we introduce a perturbation of the vector field of the dynamics—an intentional forcing term—that attracts the system toward a desired coordination pattern. This effectively turns the HDC into a virtual teacher. A key conceptual aspect is that intentional information acts in the same space as the collective variables that define the coordination patterns themselves (39). Thus, the HDC is now composed of three components (Eq. 8): the original nonlinear oscillators and nonlinear coupling of the HKB model plus the Schöner–Kelso intentional forcing term, which specifies a required relative phase,

$$\dot{\phi} = a \sin(\phi) + 2b \sin(2\phi) + c \sin(\psi - \phi), \quad [8]$$

where  $\phi$  is the relative phase,  $\psi$  is the intended or required relative phase which can take on any value between  $-\pi$  and  $+\pi$ , and  $c$  is the strength of the intentional coupling.

The intentional coupling term  $C_{int}$  is then adapted to the unidimensional component equation form (see *SI Appendix* for details):

$$C_{int} = -c(\cos(\psi)(\dot{x} - \dot{y}) + \sin(\psi)\omega y). \quad [9]$$

The higher the absolute value of  $C_{int}$ , the stronger the intention, i.e., the stronger the attraction toward the relative phase required by the VP. The benefit of this formulation is that the human can be guided to coordinate with the VP at any arbitrary relative phase (including those foreign to his or her behavioral repertoire), thereby endowing the HDC with teaching or training capabilities.



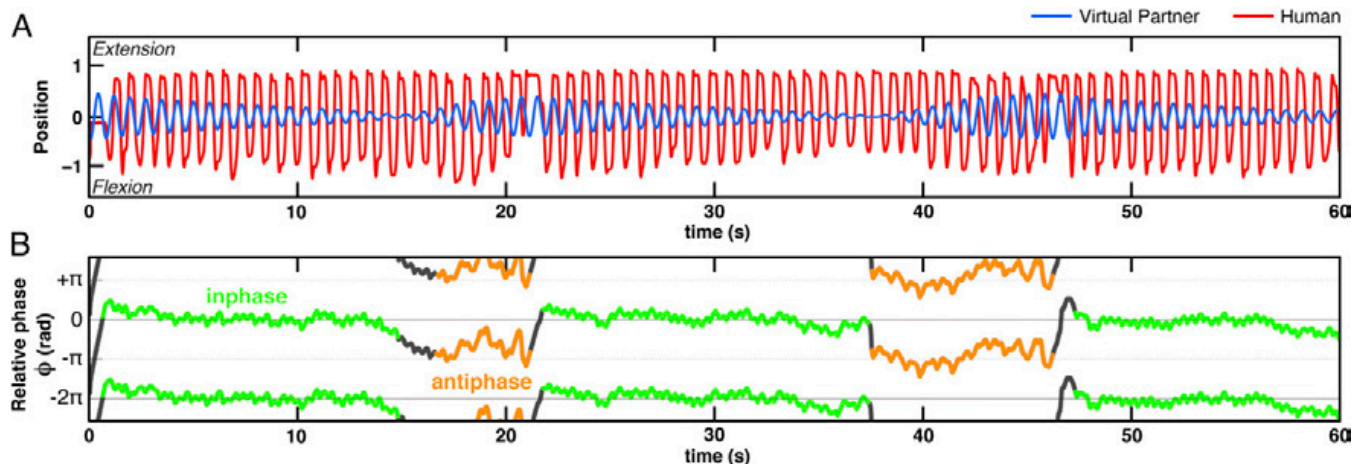


**Fig. 3.** The HDC in which the VP is governed by the HKB model (11). (A) Time series of interaction between VP (blue) and human movement (red). The parameters of the VP are set to coordinate antiphase, whereas the human is instructed to coordinate inphase. The goals of the VP and the human are thus placed in conflict. (B) Relative phase ( $\phi$ ) plot corresponding to A, showing inphase (green) to antiphase (orange) transitions between VP and human.

is directly manipulable in the HDC—is a key factor underlying accurate agency attribution (see also refs. 44 and 45).

**HDC 2: Discrete Behavior.** Interaction between a human subject and a VP governed by the excitator equations leads to three main regimes (Fig. 4): monostable (rapid ballistic movements from a steady-state posture), bistable (discrete movements from one state to another), and limit cycle (continuous rhythmic movements). Monostable coordination of human and VP is shown in Fig. 4A. Between periods of rest with the finger extended, the human subject performs brisk discrete flexion movements at will. Note how the VP coordinates and follows these discrete events. Fig. 4B shows the corresponding phase flow (in black). The nullclines (green and magenta) have a single intersection, which creates a unique fixed-point attractor: The phase flow is organized around this attractive state. Bistable coordination of human and VP is shown in Fig. 4C. The human switches at will between flexion and extension; the VP again coordinates. Note in Fig. 4D that the nullclines now intersect thrice, creating two fixed-point attractors, supporting the bistable regime. Coupled limit cycle behavior of human and VP is shown in Fig. 4E. Notice how, after an initial transient period, the continuous movements of both partners become coordinated. In Fig. 4F, the attractor at the intersection of the nullclines is unstable repelling the flow away from the origin onto a stable attracting limit cycle. The VP *qua* excitator dynamics follows the limit cycle around this unstable fixed point as seen by the dense accretion of the phase flow (in black).

The Jirsa–Kelso equations also contain a term  $I$ , which is nonautonomous in a mathematical sense and allows modification of the flow in the phase space according to an external input. When human movement is fed in as a variable, the HDC dynamics can be continuously modulated, leading to spontaneous transitions between the three main regimes (Fig. 5). Notice that the VP does not require any external intervention to tune its parameters at the (unpredictable) onset of the transition: It is able to switch spontaneously between discrete and continuous behavior just like the human participant. Thus, embedding the excitator as a VP into the HDC enables the behavioral repertoire of the dyad to be expanded and studied parametrically using a single dynamical scheme.

**HDC 3: Adaptive Behavior.** Fig. 6 illustrates the interaction between a human participant and an adaptive VP (with its internal dynamics here based on the excitator; Table 1). In Fig. 6A, the human is initially entrained to an auditory metronome at 1 Hz while looking

at a blank screen with a fixation cross. At time  $t = 0$ , the VP appears on the screen and the human is asked to accelerate his/her pace and to stop at will. Notice (i) how the VP, after an initial lag, adapts its pace and enters into inphase coordination with the human; and (ii) that the VP successfully adapts to large changes in human movement frequency. Fig. 6B displays the dynamics of the movement frequency for both human and VPs (red and blue dots, respectively) as well as the parameter dynamics of the HDC (dashed blue line). Note how the internal frequency of the HDC is updated at each cycle and, in the absence of human rhythmic movement, goes back to the preferred frequency  $\omega_0$ . As a result of phase coordination, the instantaneous frequency at the behavioral level is not required to match the internal frequency. It is worth noting that any constant in the equations of a given model can be turned into a variable, giving rise to parameter dynamics. This expands the behavioral model while preserving the original model (i.e., with fixed parameters) when the parameter dynamics is kept constant (e.g., in Eq. 7, with  $\kappa = \nu = 0$ ). Adding a third dimension to the HDC leads to a less predictable dynamics that may be associated with the chaotic regimes that are typical of 3D dynamical systems (46–48).

**HDC 4: Directed Behavior.** Fig. 7A shows the movement trajectory of a human and a VP *qua* the virtual teacher—HKB with the intentional term of Eq. 9. The relative phase  $\psi$  specified by the virtual teacher is  $\pi/2$ : The strength of the intention  $c$ , initially fixed to 1 falls to 0 after 5 s. Notice that the coordination pattern is initially sustained according to the intention of the virtual teacher, despite its intrinsic instability in most naïve subjects (49). Interestingly, when intentional forcing is turned off, the coordination pattern changes but does not return completely to inphase. This finding suggests that specifying particular patterns of coordination may lead to persistent effects in human participants. Moreover, it appears that such new behavioral patterns can be appended to the preexisting repertoire of the human as a result of interaction with a virtual teacher (see also refs. 35, 49, and 50). As illustrated in Fig. 7B, the HDC allows one to specify particular patterns of coordination for the human to learn, hence opening up a principled approach to computer-assisted learning and rehabilitation.

## Discussion

We have shown how an electrophysiological tool, the dynamic clamp, can be scaled up from neurons to people, giving birth to the paradigm of the HDC. In this paradigm a human interacts in real time with a computationally implemented theoretical model

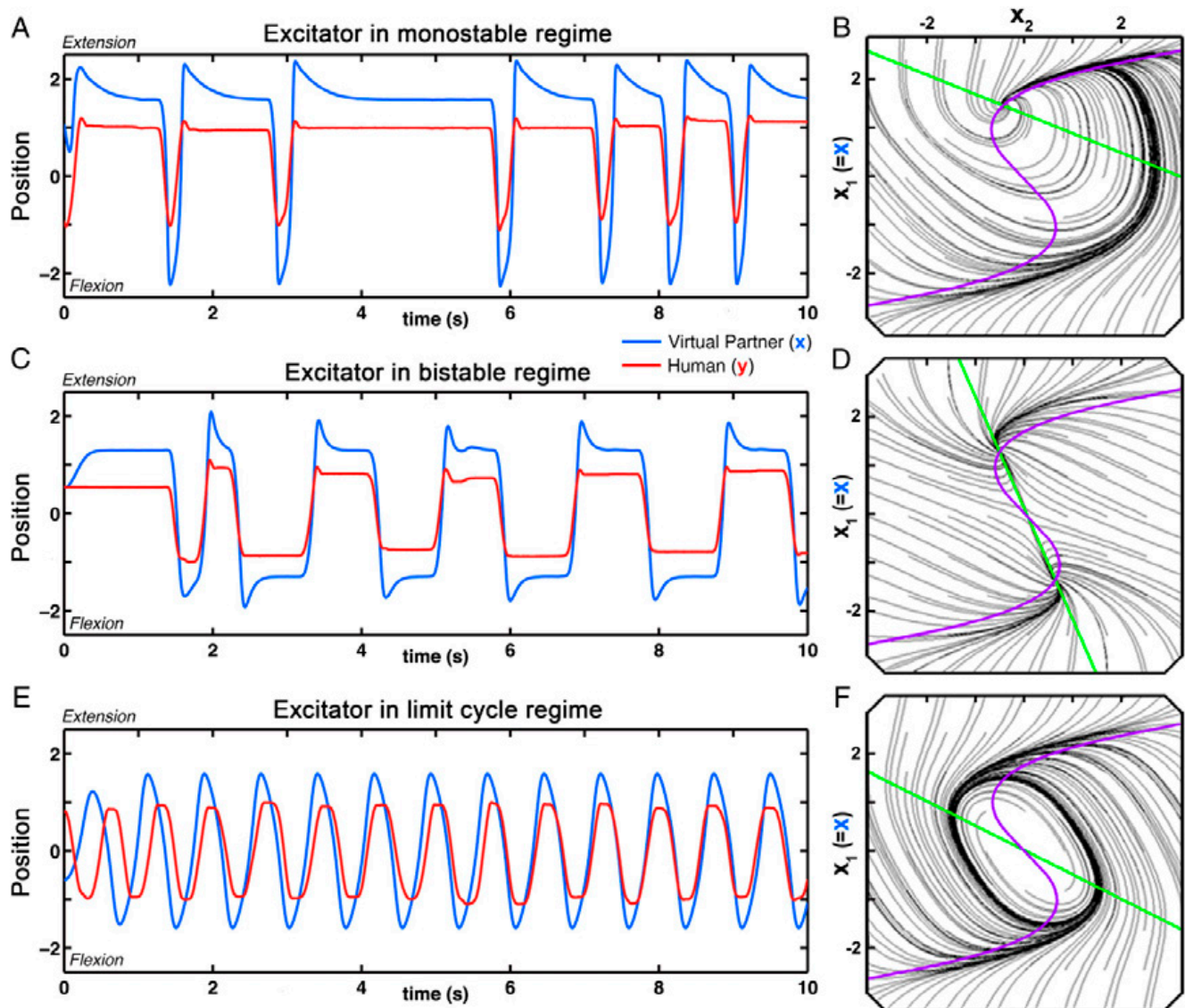


**Fig. 4.** The HDC in which the VP is governed by the Jirsa–Kelso excitator model (15) of rhythmic and discrete movement generation. (A, C, and E) Time series of reciprocal interaction between a human (red) and the VP (blue). Human is leading; VP is following. (B, D, and F) Related phase space showing nullclines (green and magenta) and phase flows (black). Notice how the angle and location ( $a$  and  $b$ ) of the green nullcline in relation to the one in magenta—the cubic curve which remains fixed—dictates the VP dynamics. (A and B) Monostable regime: The human is instructed to produce discrete movements at will and then return to rest. Parameters of the excitator-based VP:  $a = 1.3$ ;  $b = 1$ ;  $A = 0.1$ ;  $B = 0.25$ ;  $\tau = 0.1$ ;  $\omega = 1.5$ . (C and D) Bistable regime: The human is instructed to switch rapidly between flexion and extension at will. Parameters of the VP:  $a = 0$ ;  $b = 2.3$ ;  $A = 0.1$ ;  $B = 0.25$ ;  $\tau = 0.1$ ;  $\omega = 1.5$ . (E and F) Limit cycle regime: The participant is asked to move his or her finger continuously at a chosen frequency. Parameters of the VP:  $a = 0$ ;  $b = 0.5$ ;  $A = 1.5$ ;  $B = -0.1$ ;  $\tau = 1$ ;  $\omega = 1.5$ .

of him- or herself called a VP (24). Initial work demonstrated the feasibility of an HDC for coordination of rhythmic movements through the embedding of the HKB model. Experiments showed that the range of social interactions is much richer as a result of bidirectional coupling. Modifying human action in real time, even as the human is modifying the VP uncovered unexpected behaviors—the theoretical significance of which became clear only after the fact. Subsequently, the HDC was extended beyond the HKB model to explore mutual interaction in a variety of behavioral contexts. We developed a methodology for expanding the behavioral repertoire of the VP to include discrete and rhythmic movements, frequency adaptation, and intentional or environmental forcing of specific coordination patterns (Table 1). This process of generalization and resulting findings indicates how the HDC may be exploited as a general paradigm to investigate social in-

teractions. In all of the behavioral contexts explored through the HDC models, the VP could be made to behave in a manner that was appropriate to live human social interactions, coordinating, following, adapting, and teaching. This was achieved without overspecifying what behavior the VP should adopt and when it should adopt it. Instead, the VP tended to mirror the human's intrinsic behavioral repertoire; a suitable coupling provided the interaction necessary to produce patterns of social coordination. The latter were neither the product of the VP's nor the sole outcome of the human's behavioral dispositions, but rather a truly emergent collective pattern that resulted from their interaction.

**An Experimental Tool.** The expansion of the behavioral repertoire—and the strategy behind the development of the HDC—consists of implementing principle-based, empirically verified models that

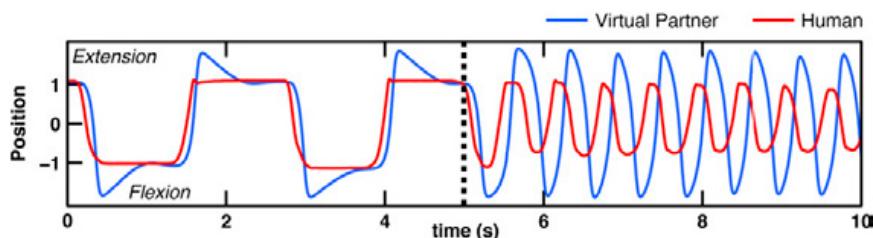


**Fig. 5.** Transitions between discrete and continuous behavior in the HDC. Here the VP is governed by the Jirsa–Kelso excitator model (15) with human position  $y$  assigned to the input  $I$ . Time series of reciprocal interaction between a human (red) and the VP (blue). Human is leading; VP is following. The human is initially instructed to move briskly between flexion and extension, pausing in-between and then, at will, to switch to producing continuous rhythmic movement. Here the transition occurs at the dashed line. Parameters of the VP:  $a = 0$ ;  $b = 0$ ;  $A = 0.5$ ;  $B = 0.025$ ;  $\tau = 1$ ;  $\omega = 1.6$ .

approximate the functionally relevant dynamics of human behavior for specific tasks and contexts. The HDC paradigm is open to any sensory modality, and may be adapted to any behavioral task. Moreover, a wide variety of processes such as the recruitment and annihilation of biomechanical degrees of freedom (51), parametric stabilization (38), sensory anchoring (37), and so forth, can be incorporated into the HDC. It seems possible that the same approach can be extended to other situations such as gaze interaction (52), imitation games (53, 54), and game theory (55), to name a few.

Neuroscientists have also recently stressed that a fine-grained analysis of the neural dynamics of social interaction is still missing, forming as it were the “dark matter” of social neuroscience (56). One of our motivations in designing the HDC was to create a tool for rigorous investigations of the neurophysiological basis of social interactions. The HDC balances ecological validity with the constraints of neuroimaging (9) by allowing full control of chosen parameters from one of the interacting agents, while at the same time preserving interaction and reciprocity. It thus may become a tool for the neurobehavioral investigation of social behavior, especially for uncovering essential nonlinearities in social behavior such as turn taking, transitions between cooperation and competition, and the neural underpinnings of attribution of intention in interactive contexts (24, 43).

**Theoretical Potential.** The main proviso for further extensions of the HDC is the availability of good, preferably empirically grounded, theoretical models. Such models can be combined to produce more complex behavior, along the lines of previous modeling work, e.g., on handwriting (57). Changes to the same system with time-varying parameters can be extended to sequences of different structures and to multiple levels (58). The next logical step in the extension of the HDC is to endow it with an explicit neural dynamics. Integrating neural and behavioral modeling in a common scheme requires tackling coordination among multiple levels (25). We have shown in the present work how parameter dynamics provides an efficient way to create behavior on multiple time scales, completely in accordance with Hebbian and synaptic plasticity (18, 35).

Besides an extensive body of work at the behavioral level, extension of the HKB model using neural oscillators has been undertaken (59–61). Theoretical research has explicitly derived the HKB equations from neural field models (e.g., refs. 25 and 62) and demonstrated the biophysical relevance of the original HKB coupling (63). The second HDC was based on the excitator (15), a model that is also biologically based, homologous to the FitzHugh–Nagumo model of nerve cell excitation (64). The excitator model has been used to uncover explanatory relationships between the stability of bimanual coordination patterns and interhemispheric delays in the cerebral cortex (65). Such converging efforts suggest that endowing the HDC with a model of a brain is

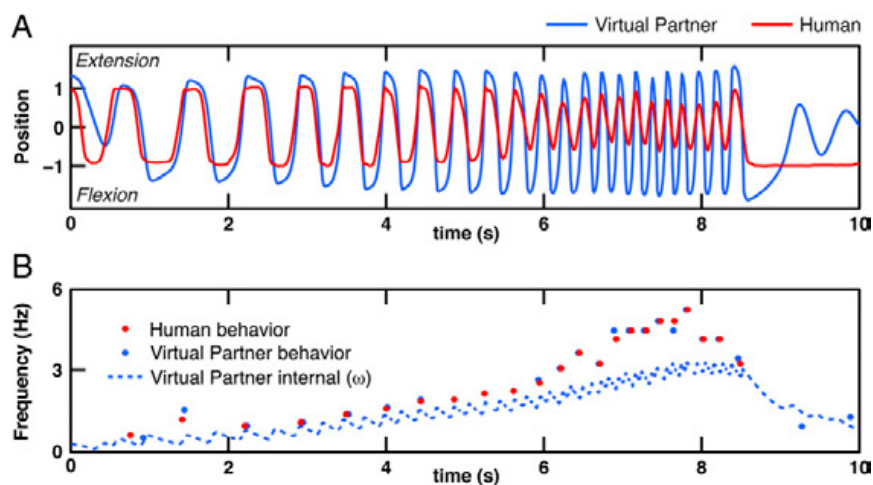


**Fig. 6.** Adaptation and parameter dynamics in the HDC. (A) Time series of interaction between an excitator as a VP (blue) adapting its pace to a human participant (red). Human is leading the interaction; VP is following. (B) Related dynamics of the intrinsic frequency parameter ( $\omega$ ) of the VP (dashed blue) compared with the dynamics of human and VP's instantaneous frequency (red and blue dots, respectively). Notice how the intrinsic frequency of the VP is updated at each cycle and how the parameter dynamics exhibits inertia after the human stops moving. When the latter occurs, frequency adaptation ceases and the VP returns to its preferred frequency following the damping part of Eq. 7. Parameters of the VP:  $a = 0$ ;  $b = 0$ ;  $A = 1$ ;  $B = -0.2$ ;  $\tau = 0.1$ ;  $\omega_0 = 1$ ;  $\kappa = 1$ ;  $\nu = 1$ .

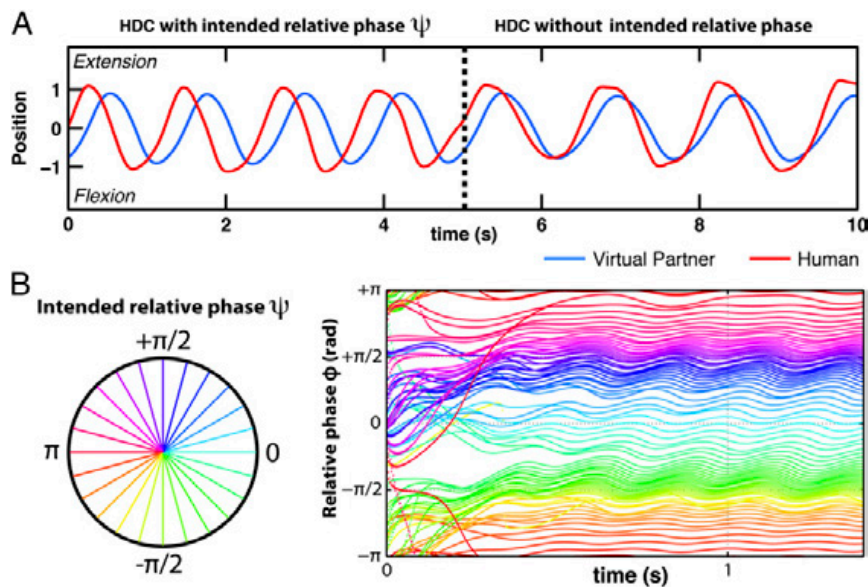


**Fig. 7.** The HDC with intentional forcing. (A) Example of interaction between a human (red) and a VP or teacher (blue) following the Schönner–Kelso (19) model of intentional behavioral change. The VP is initially driving the interaction with an intended relative phase of  $\psi = \pi/2$  ( $c = 1$ ) and ceases this behavior at the dashed line ( $c = 0$ ). Note the persistence of a slight delay near inphase after the dashed line, a remnant of the previous collective behavior imposed by the VP. Parameters of the VP:  $a = 0.641$ ;  $b = 0.00709$ ;  $A = 0.12$ ;  $B = 0.025$ ;  $\omega = 1$ . (B) Simulation of different relative phase evolutions in time for random initial conditions and different intended relative phases  $\psi$  indicated by the color wheel.

not beyond reach. Earlier work in robotics has meshed together living, electronic, and simulated components (66–68) and dynamical models such as HKB have been incorporated into robots for sensorimotor control (69, 70) and interrobot interactions (71). To achieve a desirable degree of realism, the architecture of a neurally grounded HDC may take inspiration from human connectomics (72–75). Using such an approach, Dumas et al. (76) already designed a dyadic model of two interacting brains, in good agreement with empirical evidence at both neural and social levels (77). Fully embedding a connectome with Hebbian or Hebbian-like rules in the HDC might allow testing hypotheses regarding the emergence of a mirror neuron system (78), and advance our understanding of learning, language, and their social foundations (79).

## Conclusion

The HDC offers a way to bring mind, brain, and machine together through behavior. Under such a framework, we have shown that it is possible to unify and generalize diverse functions and tasks. The approach is principled: Each new version of the HDC carries the mathematics of all previous versions (Table 1). As long as there is a medium for two-way interaction, a deeper understanding of both the model and what the model is pur-

ported to be of become possible. Once coupled bidirectionally to an unconstrained, open dynamical system like a human being, HDC's behavioral repertoire becomes much richer—in a manner akin, perhaps, to the way human behavior develops and gains depth through social interactions. In experiments, the richness of HDC behavior already led to unsolicited verbal reactions by human subjects, e.g., attribution of agency to the VP (24). Such spontaneous expressions suggest that the HDC may qualify as a Turing test of humanness (80), even surpassing its original scope. The Turing test implies only that judges are unable to tell if an agent is a human or a machine, and as such says nothing about the genuineness of the path toward that decision. Here, the HDC is a tool to test hypotheses and gain understanding about how humans interact with each other as well as with machines. In the HDC paradigm, exploration of the machine's behavior may be viewed as an exploration of us as well.

**ACKNOWLEDGMENTS.** We thank Armin Fuchs for insightful discussions about dynamical systems and the reviewers for their excellent suggestions to revise the paper. G.D. thanks Célya Gruson-Daniel for support. This work was supported by grants from the National Institute of Mental Health (MH080838), the National Science Foundation (BCS0826897), the US Office of Naval Research (N000140910527), the Chaire d'Excellence Pierre de Fermat, and the Davimos Family Endowment for Excellence in Science.

- Prinz AA, Abbott LF, Marder E (2004) The dynamic clamp comes of age. *Trends Neurosci* 27(4):218–224.
- Sharp AA, Abbott LF, Marder E (1992) Artificial electrical synapses in oscillatory networks. *J Neurophysiol* 67(6):1691–1694.
- Hodgkin AL, Huxley AF (1952) A quantitative description of membrane current and its application to conduction and excitation in nerve. *J Physiol* 117(4):500–544.
- Hutcheon B, Miura RM, Pui E (1996) Models of subthreshold membrane resonance in neocortical neurons. *J Neurophysiol* 76(2):698–714.
- Turrigiano GG, Marder E, Abbott LF (1996) Cellular short-term memory from a slow potassium conductance. *J Neurophysiol* 75(2):963–966.
- Ma M, Koester J (1996) The role of K<sup>+</sup> currents in frequency-dependent spike broadening in Aplysia R20 neurons: A dynamic-clamp analysis. *J Neurosci* 16(13):4089–4101.
- Hughes SW, Cope DW, Tóth TI, Williams SR, Crunelli V (1999) All thalamocortical neurones possess a T-type Ca<sup>2+</sup> 'window' current that enables the expression of bistability-mediated activities. *J Physiol* 517(Pt 3):805–815.
- Manor Y, Nadim F (2001) Frequency regulation demonstrated by coupling a model and a biological neuron. *Neurocomputing* 38–40:269–278.
- Hari R, Kujala MV (2009) Brain basis of human social interaction: From concepts to brain imaging. *Physiol Rev* 89(2):453–479.
- Kelso JAS (2009) Coordination dynamics. *Encyclopedia of Complexity and System Science*, ed Meyers RA (Springer, Berlin), pp 1537–1564.
- Haken H, Kelso JAS, Bunz H (1985) A theoretical model of phase transitions in human hand movements. *Biol Cybern* 51(5):347–356.
- Fuchs A (2013) *Nonlinear Dynamics in Complex Systems: Theory and Applications for the Life, Neuro- and Natural Sciences* (Springer, Heidelberg).
- Huys R, Jirsa VK, eds (2010) *Nonlinear Dynamics in Human Behavior* (Springer, Berlin).
- Huys R, Perdikis D, Jirsa VK (2014) Functional architectures and structured flows on manifolds: A dynamical framework for motor behavior. *Psychol Rev*, in press.
- Jirsa VK, Kelso JAS (2005) The excitator as a minimal model for the coordination dynamics of discrete and rhythmic movement generation. *J Mot Behav* 37(1):35–51.
- Fink PW, Kelso JAS, Jirsa VK (2009) Perturbation-induced false starts as a test of the Jirsa–Kelso excitator model. *J Mot Behav* 41(2):147–157.
- Saltzman EL, Munhall KG (1992) Skill acquisition and development: The roles of state-, parameter, and graph dynamics. *J Mot Behav* 24(1):49–57.

18. Righetti L, Buchli J, Ijspeert AJ (2009) Adaptive frequency oscillators and applications. *The Open Cybernetics and Systemics Journal* 3:64–69.
19. Schöner G, Kelso JAS (1988) A dynamic pattern theory of behavioral change. *J Theor Biol* 135(4):501–524.
20. Kelso JAS, Scholz JP, Schöner G (1988) Dynamics governs switching among patterns of coordination in biological movement. *Phys Lett A* 134(1):8–12.
21. Scholz JP, Kelso JAS (1990) Intentional switching between patterns of bimanual coordination depends on the intrinsic dynamics of the patterns. *J Mot Behav* 22(1):98–124.
22. De Luca C, Jantzen KJ, Comani S, Bertollo M, Kelso JAS (2010) Striatal activity during intentional switching depends on pattern stability. *J Neurosci* 30(9):3167–3174.
23. Rulkov NF, Sushchik MM, Tsimring LS, Abarbanel HDI (1995) Generalized synchronization of chaos in directionally coupled chaotic systems. *Phys Rev E Stat Phys Plasmas Fluids Relat Interdiscip Topics* 51(2):980–994.
24. Kelso JAS, de Guzman GC, Reveley C, Tognoli E (2009) Virtual Partner Interaction (VPI): Exploring novel behaviors via coordination dynamics. *PLoS ONE* 4(6):e5749.
25. Kelso JAS, Dumas G, Tognoli E (2013) Outline of a general theory of behavior and brain coordination. *Neural Netw* 37:120–131.
26. Fuchs A, Kelso JAS (2009) Movement coordination. *Encyclopedia of Complexity and System Sciences*, ed Meyers RA (Springer, Berlin), pp 5718–5736.
27. Kay BA, Kelso JAS, Saltzman EL, Schöner G (1987) Space-time behavior of single and bimanual rhythmic movements: Data and limit cycle model. *J Exp Psychol Hum Percept Perform* 13(2):178–192.
28. Beek PJ, Schmidt RC, Morris AW, Sim MY, Turvey MT (1995) Linear and nonlinear stiffness and friction in biological rhythmic movements. *Biol Cybern* 73(6):499–507.
29. Peters J, Schaal S (2006) Reinforcement learning for parameterized motor primitives. *Proceedings of the 2006 International Joint Conference on Neural Networks* (Institute of Electrical and Electronics Engineers, New York), pp 73–80.
30. Friston K (2011) What is optimal about motor control? *Neuron* 72(3):488–498.
31. Kohonen T (1982) Self-organized formation of topologically correct feature maps. *Biol Cybern* 43(1):59–69.
32. Harvey I, Di Paolo E, Wood R, Quinn M, Tuci E (2005) Evolutionary robotics: A new scientific tool for studying cognition. *Artif Life* 11(1-2):79–98.
33. Ermentrout B (1991) An adaptive model for synchrony in the firefly pteropyx malacca. *J Math Biol* 29(6):571–585.
34. Large EW, Jones MR (1999) The dynamics of attending: How people track time-varying events. *Psychol Rev* 106(1):119–159.
35. Righetti L, Buchli J, Ijspeert AJ (2006) Dynamic Hebbian learning in adaptive frequency oscillators. *Physica D* 216(2):269–281.
36. Kostrubiec V, Zanone PG, Fuchs A, Kelso JAS (2012) Beyond the blank slate: Routes to learning new coordination patterns depend on the intrinsic dynamics of the learner-experimental evidence and theoretical model. *Front Hum Neurosci* 6(222):222.
37. Fink PW, Foo P, Jirsa VK, Kelso JA (2000) Local and global stabilization of coordination by sensory information. *Exp Brain Res* 134(1):9–20.
38. Jirsa VK, Fink P, Foo P, Kelso JAS (2000) Parametric stabilization of biological coordination: A theoretical model. *J Biol Phys* 26(2):85–112.
39. Kelso JAS (1995) *Dynamic Patterns: The Self-Organization of Brain and Behavior* (MIT Press, Cambridge, MA).
40. Kelso JAS, Del Colle JD, Schöner G (1990) Action-perception as a pattern formation process. *Attention and Performance XIII*, ed Jeannerod M (Erlbaum, Hillsdale, NJ), pp 139–169.
41. Fuchs A, Jirsa VK, Haken H, Kelso JAS (1996) Extending the HKB model of coordinated movement to oscillators with different eigenfrequencies. *Biol Cybern* 74(1):21–30.
42. Dumas G (2011) Towards a two-body neuroscience. *Commun Integr Biol* 4(3):349–352.
43. Drever J, de Guzman GC, Tognoli E, Kelso JAS (2011) Agency attribution in the virtual partner paradigm. *Progress in Motor Control VIII: Recent Advances in Neural, Computational and Dynamical Approaches*, ed Riley MA (University of Cincinnati, Cincinnati).
44. Aucouturier JJ, Ikegami T (2009) The illusion of agency: Two engineering approaches to compromise autonomy and reactivity in an artificial system. *Adapt Behav* 17(5):402–420.
45. Barandiaran XE, Di Paolo E, Rohde M (2009) Defining agency: Individuality, normativity, asymmetry, and spatio-temporality in action. *Adapt Behav* 17(5):367–386.
46. Neuringer A, Voss C (1993) Approximating chaotic behavior. *Psychol Sci* 4(2):113–119.
47. Crutchfield JP, Farmer JD, Packard NH, Shaw RS (1986) Chaos. *Sci Am* 254(12):46–57.
48. Strogatz SH (2008) *Nonlinear Dynamics and Chaos* (Westview Press, Cambridge, MA).
49. Zanone PG, Kelso JAS (1992) Evolution of behavioral attractors with learning: Non-equilibrium phase transitions. *J Exp Psychol Hum Percept Perform* 18(2):403–421.
50. Howard IS, Ingram JN, Kording KP, Wolpert DM (2009) Statistics of natural movements are reflected in motor errors. *J Neurophysiol* 102(3):1902–1910.
51. Kelso JAS, Buchanan JJ, DeGuzman GC, Ding M (1993) Spontaneous recruitment and annihilation of degrees of freedom in biological coordination. *Phys Lett A* 179(4-5):364–368.
52. Pfeiffer UJ, Timmermans B, Bente G, Vogeley K, Schilbach L (2011) A non-verbal Turing test: Differentiating mind from machine in gaze-based social interaction. *PLoS ONE* 6(11):e27591.
53. Auvray M, Lenay C, Stewart J (2008) Perceptual interactions in a minimalist virtual environment. *New Ideas Psychol* 27(1):32–47.
54. Froese T, Iizuka H, Ikegami T (2014) Embodied social interaction constitutes social cognition in pairs of humans: A minimalist virtual reality experiment. *Sci Rep*, 10.1038/srep03672.
55. West RL, Lebiere C (2001) Simple games as dynamic, coupled systems: Randomness and other emergent properties. *Cogn Syst Res* 1(4):221–239.
56. Schilbach L, et al. (2013) Toward a second-person neuroscience. *Behav Brain Sci* 36(4):393–414.
57. Perdikis D, Huys R, Jirsa VK (2011) Time scale hierarchies in the functional organization of complex behaviors. *PLoS Comput Biol* 7(9):e1002198.
58. Minati G (2012) Introduction to the meta-structures project: Prospective applications. *World Futures* 68(8):558–574.
59. Fuchs A, Jirsa VK, Kelso JAS (2000) Theory of the relation between human brain activity (MEG) and hand movements. *Neuroimage* 11(5 Pt 1):359–369.
60. Nagashino H, Kelso JAS (1992) Phase transitions in oscillatory neural networks. *Artificial Neural Networks* 1710:279–287.
61. Beek PJ, Peper CE, Daffertshofer A (2002) Modeling rhythmic interlimb coordination: Beyond the Haken-Kelso-Bunz model. *Brain Cogn* 48(1):149–165.
62. Jirsa VK, Fuchs A, Kelso JAS (1998) Connecting cortical and behavioral dynamics: Bimanual coordination. *Neural Comput* 10(8):2019–2045.
63. Jirsa VK, Friedrich R, Haken H, Kelso JAS (1994) A theoretical model of phase transitions in the human brain. *Biol Cybern* 71(1):27–35.
64. Fitzhugh R (1961) Impulses and physiological states in theoretical models of nerve membrane. *Biophys J* 1(6):445–466.
65. Banerjee A, Jirsa VK (2007) How do neural connectivity and time delays influence bimanual coordination? *Biol Cybern* 96(2):265–278.
66. Demarse TB, Wagenaar DA, Blau AW, Potter SM (2001) The neurally controlled animat: Biological brains acting with simulated bodies. *Auton Robots* 11(3):305–310.
67. Kiss IZ, Rusin CG, Kori H, Hudson JL (2007) Engineering complex dynamical structures: Sequential patterns and desynchronization. *Science* 316(5833):1886–1889.
68. Yamashita Y, Tani J (2008) Emergence of functional hierarchy in a multiple timescale neural network model: A humanoid robot experiment. *PLoS Comput Biol* 4(11):e1000220.
69. Santos B, Barandiaran X, Husbands P, Aguilera M, Bedia M (2013) Sensorimotor coordination and metastability in a situated HKB model. *Connect Sci* 24(4):143–161.
70. Aguilera M, Bedia MG, Santos BA, Barandiaran XE (2013) The situated HKB model: How sensorimotor spatial coupling can alter oscillatory brain dynamics. *Front Comput Neurosci* 7:117.
71. Revel A, Andry P (2009) Emergence of structured interactions: From a theoretical model to pragmatic robotics. *Neural Netw* 22(2):116–125.
72. Sporns O, Tononi G, Kötter R (2005) The human connectome: A structural description of the human brain. *PLoS Comput Biol* 1(4):e42.
73. Larson-Prior LJ, et al.; WU-Minn HCP Consortium (2013) Adding dynamics to the Human Connectome Project with MEG. *Neuroimage* 80:190–201.
74. Izhikevich EM, Edelman GM (2008) Large-scale model of mammalian thalamocortical systems. *Proc Natl Acad Sci USA* 105(9):3593–3598.
75. Jirsa VK, Sporns O, Breakspear M, Deco G, McIntosh AR (2010) Towards the virtual brain: Network modeling of the intact and the damaged brain. *Arch Ital Biol* 148(3):189–205.
76. Dumas G, Chavez M, Nadel J, Martinierie J (2012) Anatomical connectivity influences both intra- and inter-brain synchronizations. *PLoS ONE* 7(5):e36414.
77. Dumas G, Nadel J, Soussignan R, Martinierie J, Garnero L (2010) Inter-brain synchronization during social interaction. *PLoS ONE* 5(8):e12166.
78. Keysers C, Perrett DI (2004) Demystifying social cognition: A Hebbian perspective. *Trends Cogn Sci* 8(11):501–507.
79. Billard A, Arbib M (2002) Mirror neurons and the neural basis for learning by imitation. *Mirror Neurons and the Evolution of Brain and Language, Advances in Consciousness Research*, eds Stamenov M, Gallese V (John Benjamins Publishing Co, Amsterdam), Vol 42, pp 343–352.
80. Turing AM (1950) Computing machinery and intelligence. *Mind* 59(236):433–460.

# Supporting Information

Dumas et al. 10.1073/pnas.1407486111

## SI Appendix

**Adaptation of the Schöner–Kelso Model.** We adapt the Schöner–Kelso Model (1) to the component level for any intended relative phase. A coupling term is introduced at the component level of the Haken–Kelso–Bunz (HKB) model (2), which intentionally stabilizes a specific relative phase  $\psi$ . For an oscillator 1 coupled with an oscillator 2,

$$C_{int} = -C(\cos(\psi)(\dot{x}_1 - \dot{x}_2) + \sin(\psi)\omega x_2),$$

where  $x_i$  and  $\dot{x}_i$  stand for position and velocity of oscillator  $i$ , respectively, and  $\omega$  is the frequency.

**Demonstration.** For more details, see the derivation of HKB in Fuchs (3).

Using  $x_j(t) = 2r \cos(\omega t + \phi_j(t)) = r(e^{i\phi_j} e^{i\omega t} + e^{-i\phi_j} e^{-i\omega t})$ , we have

$$C_{int} = -C(\cos(\psi)ir\omega(e^{i\phi_1} e^{i\omega t} - e^{-i\phi_1} e^{-i\omega t} - e^{i\phi_2} e^{i\omega t} + e^{-i\phi_2} e^{-i\omega t}) + \sin(\psi)r\omega(e^{i\phi_2} e^{i\omega t} - e^{-i\phi_2} e^{-i\omega t})).$$

Multiplying the HKB oscillator part and this coupling part by  $e^{-i\phi_1} e^{-i\omega t}$ ,

$$C_{int} = -Cr\omega \left( \cos(\psi)i \left( 1 - e^{-i2\phi_1} e^{-i2\omega t} - e^{i(\phi_2 - \phi_1)} + e^{-i(\phi_2 + \phi_1)} e^{-i2\omega t} \right) + \sin(\psi) \left( e^{i(\phi_2 - \phi_1)} - e^{-i(\phi_2 + \phi_1)} e^{-i2\omega t} \right) \right).$$

The rotating wave approximation gives

$$C_{int} = -Cr\omega(\cos(\psi)i(1 - e^{-i\varphi}) + \sin(\psi)(e^{-i\varphi})),$$

where  $\varphi = \phi_2 - \phi_1$  is the relative phase.

For the other oscillator,  $\varphi = -\varphi$  and  $\psi = -\psi$ .

The difference of the two sets of equations gives

$$-2r\omega\dot{\varphi} = -Cr\omega(\cos(\psi)i(e^{i\varphi} - e^{-i\varphi}) + \sin(\psi)(e^{-i\varphi} + e^{i\varphi}))$$

$$\dot{\varphi} = -C \left( \cos(\psi) \left( \frac{e^{i\varphi} - e^{-i\varphi}}{2i} \right) + \sin(\psi) \left( \frac{e^{i\varphi} + e^{-i\varphi}}{-2} \right) \right)$$

$$\dot{\varphi} = -C(\cos(\psi)\sin(\varphi) - \sin(\psi)\cos(\varphi)).$$

And thus

$$\dot{\varphi} = -C \sin(\varphi - \psi).$$

- Schöner G, Kelso JAS (1988) A dynamic pattern theory of behavioral change. *J Theor Biol* 135(4):501–524.
- Haken H, Kelso JAS, Bunz H (1985) A theoretical model of phase transitions in human hand movements. *Biol Cybern* 51(5):347–356.

- Fuchs A (2013) *Nonlinear Dynamics in Complex Systems: Theory and Applications for the Life, Neuro- and Natural Sciences* (Springer, Heidelberg).